Journal of Materials Chemistry B

ROYAL SOCIETY OF CHEMISTRY

PAPER

View Article Online
View Journal

Cite this: DOI: 10.1039/d5tb02538a

Hemoglobin-based oxygen carriers with antioxidant properties

Tanmay Salvi, Asim Khan, Peyton Dickerson, Griffin J. Beyer and Andre F. Palmer*

Hemoglobin (Hb)-based oxygen carriers (HBOCs) are being investigated as therapeutics for the treatment of hemorrhagic shock, when red blood cells (RBCs) are unavailable. Researchers have investigated different techniques to impart antioxidant properties to HBOCs, in order to mitigate oxidative damage observed after hemorrhagic shock resuscitation. In our previous work, we have investigated the coating of Hb with polydopamine (PDA) and have shown that PDA-coated Hb exhibits antioxidant properties while retaining its oxygen transport properties. Since the PDA coating is biodegradable and cell-free Hb in circulation is toxic, in our current study, we explore PDA coating of tense (T-) and relaxed (R-) state polymerized human hemoglobin (PolyHb). Similar to our previous study on PDA coating of CO-bound human Hb, CO binding of T- and R-state PolyHb significantly reduced metHb formation of the PDA coated PolyHb. PDA coating of PolyHb resulted in enhanced antioxidant properties of PDA–PolyHb as measured by the reducing power, radical scavenging, ferryl oxidation, and catalase activity. T-state PolyHb demonstrated moderate changes in O_2 transport properties after PDA coating, with both T- and R-state PolyHb exhibiting higher auto-oxidation rates after PDA coating. A slight increase in hydrodynamic diameter and a moderate decrease in thermal stability for both PDA-coated PolyHbs were observed compared to the precursor PolyHbs. T- and R-state PDA-coated PolyHb show promise as potential oxygen carriers with antioxidant properties, yet further optimization is needed to limit changes in oxygen transport properties.

Received 14th November 2025,
Accepted 27th May 2026

DOI: 10.1039/d5tb02538a

rsc.li/materials-b

1. Introduction

Red blood cells (RBCs) are the gold standard for blood transfusion, since they are the physiological entity responsible for transporting oxygen in the human body. However, there are certain limitations to their use, including their short *ex vivo* storage stability (42 days), which is highly dependent on blood donation rates. RBCs are also not easily accessible in situations such as natural disasters, rural areas, and war zones.[1,2] Hemoglobin-based oxygen carriers (HBOCs) are a class of artificial oxygen carriers with the potential to overcome these limitations of RBCs.

Different types of HBOCs have been investigated in the literature, such as hemoglobin (Hb) microparticles, Hb nanoparticles, pyridoxalated Hb, polyethylene glycol (PEG) crosslinked Hb, polymerized Hb (PolyHb), zeolitic imidazolate framework-8 (ZIF-8)-encapsulated Hb, and liposome-encapsulated Hb as potential oxygen carriers.[3–8] Polymerized hemoglobin (PolyHb) is synthesized by chemical crosslinking of Hb and differs from polymers such as polyethylene in the traditional sense of the word polymer. PolyHb represents an extensively studied HBOC, with examples such as Hemopure and PolyHeme having entered Phase III clinical trials. However, adverse events such as systemic hypertension, renal failure, methemoglobinemia, and myocardial infarction were observed in patients, which led to Hemopure and PolyHeme not gaining clinical approval.[9] Later studies revealed that these adverse events were caused by the presence of cell-free Hb and lower molecular weight (MW) PolyHb species (<500 kDa) present in Hemopure and PolyHeme formulations, while PolyHb species >500 kDa did not elicit these adverse effects.[10] Thus, our group has synthesized tense (T-) and relaxed (R-) state PolyHb, bracketed between 500 kDa and 0.2 μm, at the bench scale (2 L),[11] as well as the pilot scale, yielding 200–300 g in a 30 L reactor,[12] and subsequently PEGylated these variants to create an advanced HBOC formulation with potential for diverse biomedical uses.[13] T-state PolyHb with a low oxygen affinity is suitable for hemorrhagic shock resuscitation, whereas R-state PolyHb with a high oxygen affinity is suitable for oxygenating tumor microenvironments that are severely hypoxic.[14,15]

HBOCs have an inherent potential to generate reactive oxygen species (ROS) owing to oxidative reactions of the heme

William G. Lowrie Department of Chemical and Biomolecular Engineering, The Ohio State University, Columbus, OH, USA. E-mail: palmer.351@osu.edu

group.[16] ROS can oxidize lipids, damage DNA, and result in cell death.[17] Therefore, several attempts have been made to synthesize HBOCs with antioxidant properties. For example, Dr Chang's group has developed PolyHb co-polymerized with antioxidant enzymes superoxide dismutase and catalase,[18] while Dr Hosta-Rigau's group have developed metal–phenolic network coatings to impart antioxidant properties.[19] Multiple groups, including us, have also employed an antioxidant polydopamine (PDA) coating to hHb, as an HBOC.[20–25]

In our previous work, we explored different methods of PDA-coating of hHb to understand the effect of PDA coating on the biophysical and biochemical properties of hHb. PDA coating is proven to be biodegradable, and transfusion of PDA–hHb would potentially lead to exposure of cell-free hHb, after biodegradation of the PDA coating.[26] Cell-free hHb is known to elicit hypertension by scavenging nitric oxide (NO) and cause renal failure due to hHb dimerization.[27,28] Therefore, in this work, we explore PDA coating of tense (T-) and relaxed (R-) state PolyHb as an artificial oxygen carrier with antioxidant properties. PolyHb has shown safety and efficacy as an oxygen carrier in various animal models[14,29–31] and thus, PDA–PolyHb would be a safer transfusion alternative compared to PDA–hHb.

For PDA coating of hHb, we observed that binding CO to hHb before PDA coating significantly reduced methemoglobin (metHb) formation. We also found that coating CO-bound hHb with pre-formed PDA nanoparticles (NPs) significantly reduced auto-oxidation rates but also resulted in larger-sized PDA–hHb NPs (~400 nm). We desire HBOCs to have a size <200 nm to prevent rapid clearance through the reticuloendothelial system (RES), which is achieved *via* a 0.2 μm sterile filtration step.[32] Therefore, in this work, we chose to explore PDA coating of CO-bound PolyHb, without pre-formed PDA NPs. The precursor T- and R-state PolyHbs are referred to as PolyHb-T and PolyHb-R, respectively, and their PDA-coated variants are referred to as PDA–PolyHb-T and PDA–PolyHb-R throughout the work. To compare the benefit of CO-binding on metHb reduction, we also synthesized PDA–PolyHb without CO-bound PolyHb. Biophysical and biochemical properties of PolyHb-T, PDA–PolyHb-T, PolyHb-R, and PDA–PolyHb-R were evaluated. Successful incorporation of antioxidant properties was verified using the ferric reducing antioxidant power (FRAP) assay, (2,2′-Azino-bis(3-ethylbenzothiazoline-6-sulfonic acid)) ABTS radical scavenging assay, ferryl Hb formation assay, and catalase activity assay. Oxygen transport properties were evaluated by measuring oxygen equilibrium curves, oxygen offloading kinetics, and auto-oxidation kinetics. The structural and thermal stability of the proteins were probed using circular dichroism, and protein size was measured using dynamic light scattering (DLS) and sodium dodecyl sulfate-polyacrylamide gel electrophoresis (SDS-PAGE).

2. Materials and method

2.1. Materials

Sodium dithionite ($Na_2S_2O_4$), sodium cyanoborohydride ($NaCNBH_3$), *N*-acetyl-L-cysteine (NALC, $C_5H_9NO_3S$), glutaraldehyde ($C_5H_8O_2$) (25 wt%), sodium cyanoborohydride ($NaCNBH_3$), glycine ($C_2H_5NO_2$), sodium lactate ($NaC_3H_5O_3$), and calcium chloride dihydrate ($CaCl_2{\cdot}2H_2O$) were acquired from Sigma-Aldrich (St. Louis, MO). Potassium chloride (KCl), Sodium chloride (NaCl), sodium hydroxide (NaOH), sodium phosphate monobasic (NaH_2PO_4), and sodium phosphate dibasic (Na_2HPO_4) were acquired from Fisher Scientific (Pittsburgh, PA). A 3 M Liqui-Cel EXF Series membrane gas/liquid contactor (G420 2.5 × 8) was acquired from 3 M (St. Paul, MN). 2,4,6-Tripyridyl-*S*-triazine (TPTZ) was obtained from TCI Chemicals (Portland, OR). Ultraviolet (UV) lamps (UVP Blak-Ray B-100AP) were acquired from Analytik Jena (Upland, CA).

2.2. Hb purification from human RBC

Human hemoglobin (hHb) was purified using tangential flow filtration (TFF) following established protocols.[33] Recently expired human RBC units were procured from Impact Life (Davenport, IA) and 20 units were pooled, diluted to ~20% hematocrit, and thoroughly washed through six diafiltration cycles with phosphate buffer using a 0.65 μm hollow fiber filter. The cells were then concentrated, lysed with phosphate buffer (pH 7.4) at 4 °C, and clarified by filtration on 500 kDa hollow fiber module to remove cell debris >500 kDa. The resulting hemolysate (<500 kDa), composed primarily of hHb (~98%) with trace RBC enzymes,[12] was further concentrated using a 50 kDa filter to 200–250 mg mL^{-1} and stored at −80 °C until use.

2.3. Synthesis and quantification of T- and R-state PolyHb

T- and R-state PolyHb were synthesized using methods reported in the literature.[12] Briefly, 480 g of human Hb at 20 mg mL^{-1} (Hb basis) was either fully oxygenated or deoxygenated to yield R- or T-state Hb respectively, and polymerization was performed using glutaraldehyde as a crosslinker at a 30 : 1 glutaraldehyde to Hb molar ratio at 37 °C. Sodium cyanoborohydride (Sigma-Aldrich) and glycine (Sigma-Aldrich) were used to quench the reaction at a 7 : 1 quencher : glutaraldehyde molar ratio. The resultant mixture containing cell-free Hb, low MW PolyHb species and high MW PolyHb species was purified using 0.2 μm and 500 kDa MW cutoff hollow fiber filters (Repligen) to retain high MW PolyHb (500 kDa < MW < 0.2 μm) as the final product.

2.4. PDA coating of T-, R-state PolyHb, and hHb

T- and R-state PolyHb were bound with CO using a gas–liquid contactor (3 M). To perform the PDA coating of PolyHb, 1000 mg of T- or R-state PolyHb and 321 mg dopamine-HCl were added to 132 mL of 10 mM Tris buffer (pH = 8.5) at room temperature. The reaction mixture was stirred at 500 RPM for 1 h followed by purification using TFF over a 500 kDa hollow fiber filter (Repligen) for 5 volume exchanges with 155 mM PBS (pH = 7.4). Volume exchanges were performed to buffer exchange PDA–PolyHb to a physiological pH and to remove any unreacted dopamine from the PDA–PolyHb product. The purified product was stored at −80 °C and was thawed before CO-unlocking using photolysis. The metHb content of the non-CO-bound PDA–PolyHb-T or

PDA–PolyHb-R, as well as other biophysical and biochemical properties were analyzed. To serve as a control, PDA coating of hHb was performed by implementing the method described above (PDA–hHb-13).[20]

2.5. CO-unlocking and MetHb assay

CO-unlocking was performed by photolysis of CO from the CO-bound PDA–PolyHb-T and PDA–PolyHb-R. 10 mL of CO-PDA–PolyHb at ~7 mg mL^{-1} (Hb basis) was placed in a rotating round-bottom flask at room temperature and irradiated for 5 minutes with UV light using UV lamps (UVP Blak-Ray B-100AP) in an oxygen-rich environment. CO-unlocking was confirmed by spectral changes of the samples, with the Soret peak of CO-bound proteins shifting from 418 nm to 414 nm for CO-unlocked proteins. Similarly, Q bands for the CO-bound proteins shifted from 570 nm to 576 nm for CO-unlocked proteins. The cyanomethemoglobin assay (metHb assay) was employed to quantify the total Hb concentration in the sample and metHb content using methods reported in the literature.[34]

2.6. Quantification of dopamine in PDA coating

Dopamine incorporation in the PDA coating was calculated using methods similar to our work on PDA–hHb.[20] Briefly, the mass of dopamine incorporated in the PDA coating was calculated as the difference between the mass of dopamine added to the reaction mixture and the mass of dopamine permeated during TFF purification of PDA–PolyHb. The dopamine permeated through the TFF filter was quantified using its absorbance at 280 nm and a dopamine calibration curve. The contribution of any PolyHb-CO in the permeate was estimated using its absorbance at 418 nm.

2.7. Dynamic light scattering

Dynamic light scattering (DLS) measurements were performed using a Zetasizer Pro (Malvern Panalytical Inc., Westborough, MA) at a scattering angle of 90° and at a wavelength of 637 nm for protein samples diluted to ~0.5 mg mL^{-1} in deionized water. Hydrodynamic diameter was calculated as the volume-weighted mean of the distribution. The polydispersity index (PDI) was calculated as the square of the ratio of the standard deviation of the volume-weighted distribution to the mean of the volume-weighted distribution, as represented by eqn (1).

$$\mathrm{PDI} = \left(\frac{\text{Standard deviation}}{\text{Mean}}\right)^2 \quad (1)$$

2.8. SDS-PAGE

Proteins were diluted to a concentration of 5 mg mL^{-1} and combined with tris-glycine SDS sample buffer (Novex, Carlsbad, CA) in a 1 : 1 volume ratio. 0.1 M dithiothreitol (DTT) was added to the sample mixture to induce denaturating conditions. Samples were heated to 85 °C for 10–15 minutes and 20 μL of sample solutions were loaded onto a 4–20% tris-glycine gradient gel (Invitrogen, Waltham, MA). Electrophoresis was conducted in a Mini Gel Tank system (Invitrogen) for 40 minutes at 220–225 V. Post electrophoresis, gels were stained using Coomassie blue for 20–45 minutes, followed by destaining using a solution of 60% deionized water, 30% methanol, and 10% acetic acid for 1–2 hours. Gels were imaged, and a standard molecular weight ladder was used as a reference for molecular weight analysis.

2.9. Oxygen equilibrium curve

Oxygen equilibrium curves (OECs) were measured using a Hemox Analyzer (TCS Scientific Corp., New Hope, PA) to assess the oxygen affinity and cooperativity coefficient of the proteins. Proteins were diluted to 60 μM (heme basis) in Hemox buffer, and 20 μL of additive A and antifoam agent each (TCS Scientific Corp.) were added. The P_{50}, oxygen partial pressure corresponding to 50% Hb O_2 saturation of the O_2 binding sites, and the Hill coefficient (n) were obtained by fitting the OEC data to the Hill equation and regressing the parameters.

2.10. Auto-oxidation kinetics

Auto-oxidation describes the spontaneous conversion of $HbFe^{2+}$ to $HbFe^{3+}$, and the kinetics of Hb auto-oxidation were measured by monitoring the absorbance maxima of Fe^{3+} at 630 nm, following methods reported in the literature.[35] Protein samples were diluted to 12.5 mg mL^{-1} (Hb basis) in 155 mM PBS in a 0.1 cm path length quartz cuvette, and incubated at 37 °C for 20 h. UV-visible spectra were recorded every 30 minutes and the rate constant for auto-oxidation ($k_{\text{auto-ox}}$) was obtained by fitting the rate of decrease in ferrous Hb concentration to an exponential function.

2.11. Oxygen offloading kinetics

Oxygen offloading kinetics and haptoglobin binding kinetics were studied using a SX-20 microvolume stopped-flow instrument (Applied Photophysics, Charlotte, NC). Oxygen offloading was triggered by the reaction of 1.5 mg mL^{-1} sodium dithionite with oxygenated protein samples at 12.5 μM (Hb basis). The rate of oxygen offloading was measured by monitoring the absorbance at 437.5 nm corresponding to deoxygenated Hb, over 60 seconds. At least 7 kinetics traces were fitted to a first-order rate equation to derive the rate constant for oxygen offloading ($k_{O_2,\text{off}}$).

2.12. Haptoglobin binding kinetics

The kinetics of haptoglobin (Hp) binding to the proteins was measured using stopped flow fluorescence spectroscopy. Hp at 0.25 μM was mixed with varying concentrations of proteins (5, 10, 15, 20 μM, Hb basis). The kinetics of Hp binding was measured using fluorescence quenching of Hp due to the heme group at 310 nm. Measurements at each concentration were fit to a single exponential function to obtain a pseudo-first order rate constant, k_{obs} (s^{-1}). The slope of k_{obs} *versus* protein concentration represents the bimolecular Hp binding rate constant, $k_{\text{Hp-Hb}}$ ($\mu M^{-1}\ s^{-1}$).

2.13. Ferric reducing antioxidant power (FRAP) assay

The ferric reducing antioxidant (FRAP) assay was employed to quantify the proteins' ability to reduce oxidants, by following

methods reported in the literature.[36] Briefly, a working solution was prepared by combining acetate buffer (300 mM, pH = 3.6), TPTZ solution (10 mM in 40 mM HCl), and $FeCl_3$ (20 mM) in a 10 : 1 : 1 volume ratio. 10 μL of treatments were added to 200 μL of the working solutions, and the absorbance at 593 nm was measured after incubation at 37 °C for 4 minutes. A standard curve was generated using varying concentrations of ascorbic acid as a reference treatment, and protein samples were analyzed at a concentration of 2 mg mL^{-1} (Hb basis). FRAP values for treatments were calculated by implementing eqn (2).

$$\text{Protein FRAP value}\left(\mu\text{M}\,\mu\text{g}^{-1}\text{ protein}\right) = \frac{2 \times [\text{Abs(WS + sample)} - \text{Abs(WS + PBS)} - \text{Abs(PBS + sample)}]}{10(\mu\text{L}) \times \text{sample concentration} \times \text{calibration curve slope}} \quad (2)$$

where, WS = working solution, PBS = phosphate-buffered saline.

2.14. ABTS radical scavenging assay

The ABTS radical scavenging assay, as the name suggests, measures the ability of proteins to scavenge free radicals and was performed following methods reported in the literature.[37] 7 mM ABTS was added to 4.9 mM sodium periodate ($NaIO_4$) to prepare a stock solution containing oxidized $ABTS^{\bullet}$ radicals. The stock solution was stored at room temperature for at least 14 hours before use and was diluted to yield an absorbance of 0.1–1.0 mAu at 734 nm. The assay was conducted by adding 10 μL of protein samples at 2 mg mL^{-1} to 200 μL of the working solution. A reference for the working solution (ABTS Ref) was prepared by mixing 200 μL of the working solution with 10 μL of PBS. All samples were incubated in the dark for 5 min at room temperature, after which the absorbance was measured at 734 nm. The free radical scavenging ratio of the proteins was calculated using eqn (3).

$$\text{Scavenging ratio}(\%/\mu\text{g protein}) = \frac{\text{Abs(ABTSRef)} - [\text{Abs(ABTS + sample)} - \text{Abs(PBS + sample)}]}{10(\mu\text{L}) \times \text{sample concentration} \times \text{Abs(ABTS Ref)}} \times 100 \quad (3)$$

2.15. Hydrogen peroxide mediated oxidation

The tendency of Fe in the proteins to oxidize to ferryl species (Fe^{4+}) was studied using the hydrogen peroxide mediated oxidation assay, also called the sulfHb assay, following methods reported in the literature.[38] Proteins were diluted to 60 μM (heme basis) and H_2O_2 (600 μM) was added to initiate the oxidation for 5 min at room temperature. The reaction was quenched with the addition of catalase (200 units per mL) for 1 min, followed by the addition of 2 mM sodium sulfide (Na_2S) to convert ferryl Hb to sulfated Hb (sulfHb), which is more stable. Formation of ferryl Hb was quantified by quantifying sulfHb using its absorption maximum at 620 nm and an extinction coefficient of 24 mM^{-1} cm^{-1}.

2.16. Catalase activity assay

The catalase activity assay was employed to evaluate the proteins' ability to scavenge H_2O_2 in solution following methods reported in the literature.[38] Varying concentrations of catalase (0, 1, 2, 3, 4, 5, and 10 units per mL) were incubated with 15 mM H_2O_2 for 3 minutes at room temperature, and the absorbance at 240 nm was recorded to generate a standard curve. Proteins were diluted to 2 μM (Hb basis) and analyzed similarly. Catalase activity of the protein samples was calculated by correlating the absorbance change at 240 nm with activity using the standard curve.

2.17. Circular dichroism spectroscopy

Circular dichroism (CD) spectroscopy was used to understand the effect of the PDA coating on the structure of PolyHbs. A JASCO J-815 CD spectrometer (JASCO, Easton, MD) was used to acquire CD spectra. Far-UV spectra were recorded between 190 nm and 260 nm to analyze the secondary structure of the proteins at 0.5 mg mL^{-1}. Similarly, near-UV spectra were recorded between 250 nm and 500 nm to analyze the tertiary structure of the proteins at 1.5 mg mL^{-1}. All dilutions were made in 155 mM PBS (pH = 7.4), and a quartz cell with 0.1 cm path length was used to acquire spectra. Baseline corrections were performed using 155 mM PBS (pH = 7.4), and each measurement was averaged using three scans.

2.18. Thermal stability

A JASCO J-815 CD spectrometer connected to a Peltier device for temperature control was used to evaluate the effect of PDA coating on the thermal stability of proteins. Proteins were diluted to 0.5 mg mL^{-1} in 155 mM PBS buffer (pH = 7.4) in a 0.1 cm path length quartz cuvette. The molar ellipticity at 222 nm was recorded as the temperature was increased from 20 °C to 90 °C at a rate of 2.5 °C per minute, with a 3 minute equilibration time at each step. 155 mM PBS buffer (pH = 7.4) was also used to make baseline corrections.

2.19. Safety and hazard handling

Appropriate personal protective equipments such as safety goggles, gloves, and lab coats were utilized while conducting all experiments. Hazardous chemicals including glutaraldehyde, sodium cyanoborohydride, potassium cyanide, and potassium ferricyanide were handled in a chemical fume hood and disposed following university guidelines. RBC blood bags were handled in a biosafety cabinet to mitigate the risk of blood borne pathogen exposure. Biological waste from RBC lysis and hemoglobin products were disinfected with bleach before disposal by the University's waste management division.

2.20. Statistical analysis

Statistical analyses were performed using JMP software (JMP Pro, Version 16. SAS Institute Inc., Cary, NC). Unequal variances tests were performed to assess if the groups had equal variances, and means were compared using Student's *t*-test with a significance level of 5% ($\alpha = 0.05$).

3. Results

3.1. PolyHb synthesis and purification

T- and R-state PolyHb were synthesized as described in the literature and were bound to CO using a gas/liquid contactor. T-state PolyHb had a metHb content of 4.4 ± 0.0%, whereas R-state PolyHb had a metHb content of 1.3 ± 0.1% (Fig. 1).

3.2. PDA–PolyHb synthesis and purification

The PDA coating of T- and R-state PolyHb (PolyHb-T and PolyHb-R) was performed by simultaneous addition of dopamine and PolyHb in Tris Buffer, pH = 8.5, at room temperature. The reaction mixture was stirred at 500 rpm for 1 h, followed by buffer exchange using TFF for 5 diacycles to remove unreacted dopamine in the permeate, and to buffer exchange to a physiological pH of 7.4. The PDA coating was implemented for T- and R-state PolyHb with and without CO locking.

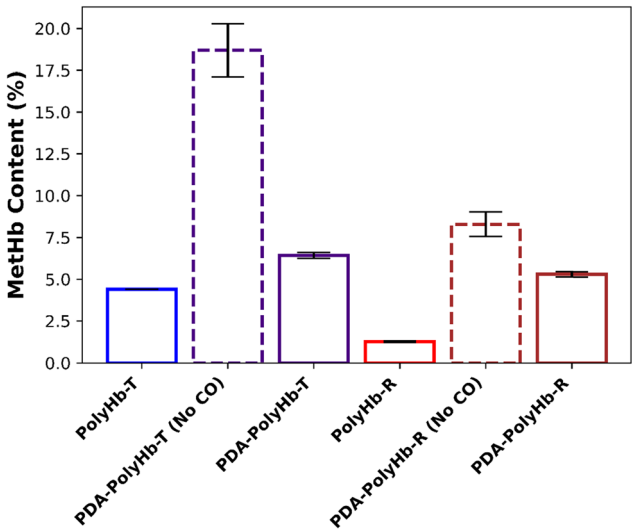

Fig. 1 MetHb content of PolyHb-T, PDA–PolyHb-T (without CO locking), PDA–PolyHb-T (with CO locking), PolyHb-R, PDA–PolyHb-R (without CO locking), and PDA–PolyHb-R (with CO locking) post synthesis.

In our study with PDA coating of hHb, we observed that CO locking hHb before PDA coating, and photolyzing off the CO (CO-unlocking) bound to the synthesized PDA–hHb resulted in a significantly lower metHb formation compared to PDA coating of hHb without CO locking.[20] For PDA coating of T- and R-state PolyHb without CO locking, we observed metHb levels of 18.7 ± 1.9% and 8.3 ± 0.9% respectively (Fig. 1). Whereas PDA coating of T- and R-state PolyHb with CO locking and unlocking, had metHb levels of 6.4 ± 0.2% and 4.8 ± 0.8% respectively (Fig. 1). Thus, CO locking significantly reduced metHb formation for PDA-coated T-state PolyHb by about 10% ($p < 0.001$), whereas the reduction in metHb content for PDA-coated R-state PolyHb because of CO locking was about 3% ($p < 0.01$).

Biophysical and biochemical properties of PDA-coated T- and R-state PolyHb with CO locking and unlocking (PDA–PolyHb-T and PDA–PolyHb-R) were analyzed along with their precursor T- and R-state PolyHbs (Table 1).

3.3. Quantification of dopamine in PDA coating

Dopamine incorporated in the PDA coating was estimated *via* a mass balance that accounted for the total mass of dopamine added to the reaction mixture, and the total mass of dopamine permeated during TFF purification of PDA–PolyHb. PDA-Poly-T and PDA-Poly-R had similar levels of dopamine in their PDA coatings ($p > 0.05$), with PDA-Poly-T having 39.7 ± 10.7 mg dopamine/g Hb and PDA-Poly-R having 41.7 ± 9.9 mg dopamine/g Hb in their respective coatings.

3.4. Dynamic light scattering (DLS)

The particle size distribution was analyzed by quantifying the hydrodynamic diameter and polydispersity index using DLS (Fig. 2). Polymerized Hbs, PolyHb-T and PolyHb-R exhibited a hydrodynamic diameter of 28.1 ± 2.7 nm and 17.2 ± 0.5 nm respectively, whereas their PDA coated variants PDA–PolyHb-T and PDA–PolyHb-R had a hydrodynamic diameter of 44.9 ± 7.0 nm and 19.1 ± 0.8 nm respectively. Both PolyHbs demonstrated a significant increase in their respective hydrodynamic

Table 1 Comprehensive biophysical and biochemical characterization of T- and R-state PolyHb, and their respective PDA-coated variants

Biophysical properties		PolyHb-T	PDA–PolyHb-T	PolyHb-R	PDA–PolyHb-R	hHb[20]	PDA–hHb-13[20]
metHb level (%)		4.4 ± 0.0^{b}	6.4 ± 0.2^{a}	1.3 ± 0.1^{d}	4.8 ± 0.8^{c}	1.0 ± 0.1^{f}	4.4 ± 0.5^{e}
Dopamine in PDA coating (mg dopamine/g Hb)		N/A	39.7 ± 10.7	N/A	41.7 ± 9.9	N/A	34.3 ± 7.1
$k_{auto\text{-}ox}$ (h^{-1})	Fast	0.0191 ± 0.0004^{b}	0.0848 ± 0.0095^{a}	0.0072 ± 0.0006^{d}	0.0201 ± 0.0003^{c}	0.008 ± 0.001^{f}	0.078 ± 0.006^{e}
	Slow	0.0191 ± 0.0004^{ns}	0.0164 ± 0.0019^{ns}	0.0072 ± 0.0006^{d}	0.0094 ± 0.0002^{c}	0.008 ± 0.001^{f}	0.078 ± 0.006^{e}
SulfHb (μM) 1 : 10 (Heme : H_2O_2)		13.0 ± 0.0^{b}	3.8 ± 0.4^{a}	1.3 ± 0.1^{ns}	1.3 ± 0.0^{ns}	0.3 ± 0.0^{f}	6.6 ± 0.4^{e}
Catalase activity (units per mL)		3.6 ± 0.5^{b}	5.2 ± 0.4^{a}	21.4 ± 2.1^{ns}	22.6 ± 0.8^{ns}	20.3 ± 0.7^{f}	4.6 ± 0.2^{e}
P_{50} (mm Hg)		34.3 ± 2.1^{b}	14.5 ± 2.3^{a}	2.6 ± 0.1^{d}	3.2 ± 0.3^{c}	14.5 ± 0.7^{f}	17.2 ± 0.9^{e}
n		1.0 ± 0.0^{ns}	0.9 ± 0.0^{ns}	1.0 ± 0.1^{ns}	1.0 ± 0.1^{ns}	2.8 ± 0.2^{f}	1.6 ± 0.0^{e}
$k_{O_2,off}$ (s^{-1})		36.5 ± 0.2^{b}	24.4 ± 1.6^{a}	14.1 ± 0.4^{ns}	15.2 ± 0.7^{ns}	41.1 ± 0.8^{ns}	41.3 ± 1.3^{ns}
$k_{Hp\text{–}Hb}$ (μM^{-1} s^{-1})		0.0058 ± 0.0007^{ns}	0.0048 ± 0.0004^{ns}	0.0040 ± 0.0001^{ns}	0.0036 ± 0.0002^{ns}	0.15 ± 0.02^{ns}	0.16 ± 0.00^{ns}
FRAP (μM μg^{-1})		10.4 ± 0.3^{b}	32.4 ± 1.3^{a}	9.3 ± 0.5^{d}	21.3 ± 1.5^{c}	14.8 ± 0.5^{f}	31.5 ± 1.1^{e}
ABTS (% μg^{-1})		1.22 ± 0.07^{b}	3.05 ± 0.12^{a}	1.06 ± 0.07^{d}	2.26 ± 0.12^{c}	1.6 ± 0.1^{f}	2.9 ± 0.1^{e}
Dia (nm)		28.1 ± 2.7^{b}	44.9 ± 7.0^{a}	17.2 ± 0.5^{d}	19.1 ± 0.8^{c}	3.7 ± 0.3^{ns}	6.0 ± 1.0^{ns}
PDI		0.14 ± 0.02^{ns}	0.65 ± 0.29^{ns}	0.13 ± 0.01^{ns}	0.49 ± 0.61^{ns}	0.05 ± 0.02^{ns}	0.02 ± 0.0^{ns}
T_m (°C)		73.9 ± 0.7^{b}	71.3 ± 0.8^{a}	78.1 ± 1.3^{ns}	76.0 ± 1.4^{ns}	65.9 ± 0.2^{f}	59.3 ± 0.2^{e}

Significantly different compared to [a] PolyHb-T. [b] PDA–PolyHb-T. [c] PolyHb-R. [d] PDA–PolyHb-R. [e] hHb. [f] PDA–hHb-13 ($p < 0.05$).

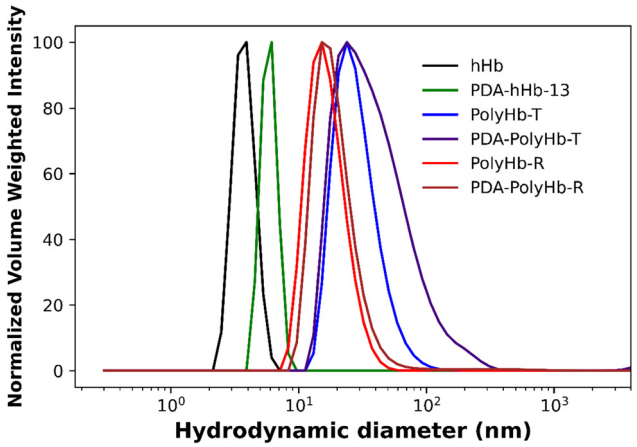

Fig. 2 Representative DLS analysis of hHb, PDA–hHb-13, PolyHb-T, PDA–PolyHb-T, PolyHb-R, PDA–PolyHb-R.

diameters due to the PDA coating ($p < 0.05$). Comparatively, hHb had an increase in its average hydrodynamic diameter upon PDA coating, increasing from 3.7 ± 0.3 nm for hHb to 6.0 ± 1.0 nm for PDA–hHb-13. However, this change was not statistically significant owing to variance from other groups.[20] The PolyHbs did not show a change in their polydispersity upon PDA coating ($p > 0.05$), with PolyHb-T, PolyHb-R, PDA–PolyHb-T, and PDA–PolyHb-R having polydispersity indices of 0.14 ± 0.0, 0.1 ± 0.0, 0.6 ± 0.3, and 0.5 ± 0.6 respectively.

3.5. SDS-PAGE

The precursor human Hb (hHb), T-state PolyHb, PDA-T-state PolyHb, R-state PolyHb, and PDA-R-state PolyHb samples were examined using SDS-PAGE under both non-denaturing (without DTT) and denaturing conditions (with DTT), as illustrated in Fig. 3A and B. Lane 1 shows the molecular weight (MW) marker, and lane 2 contains the precursor hHb. Lane 3 corresponds to the precursor T-state PolyHb, lanes 4–6 represent three independent batches of PDA-T-state PolyHb, lane 7 contains the precursor R-state PolyHb, and lanes 8–10 correspond to three batches of PDA-R-state PolyHb. All tested samples, including the precursor hHb, the precursor T- and R-state PolyHb, and their PDA-coated counterparts, displayed a band around 16 kDa, which aligns with the expected molecular weight of the α- and β-subunits of hHb. Under both gel conditions, tetrameric hHb ($\alpha_2\beta_2$) dissociated into its α/β monomeric subunits, resulting in a single, strong band due to co-migration. Weak additional bands near 30–32 kDa were also detected, most likely corresponding to trace RBC enzymes, as the hHb precursor is approximately 98% pure as reported previously in the literature.[12] Compared with the precursor hHb, both the unmodified and PDA-coated T- and R-state PolyHb samples migrated differently, displaying multiple bands indicative of a range of polymerized species. Across all PolyHb preparations, major bands were seen above 250 kDa, accompanied by several minor bands that likely represent smaller PolyHb fractions present in solution.

3.6. Oxygen equilibrium curve (OEC)

Oxygen affinity and cooperativity of the precursor hHb and PolyHbs (hHb, PolyHb-T, and PolyHb-R) and the PDA-coated variants (PDA–hHb-13, PDA–PolyHb-T, and PDA–PolyHb-R) were assessed using the Hemox Analyzer to measure the P_{50} (oxygen partial pressure at which 50% of Hb O_2 binding sites are saturated with O_2) and Hill coefficient (n) (Fig. 4). PolyHb-T had a P_{50} of 34.3 ± 2.1 mmHg, which was significantly decreased upon PDA coating ($p < 0.001$), with PDA–PolyHb-T having a P_{50} of 14.5 ± 2.3 mmHg. In contrast, PolyHb-R had a P_{50} of 2.6 ± 0.1 mmHg, which significantly increased upon PDA coating ($p < 0.05$), with PDA–PolyHb-R exhibiting a P_{50} of 3.2 ± 0.3 mmHg. The precursor hHb had a P_{50} of 14.5 ± 0.7 mmHg, which increased to 17.2 ± 0.9 mmHg upon PDA coating (PDA–hHb-13).[20] The Hill coefficients of PolyHb-T and PolyHb-R did not change significantly upon PDA coating. PolyHb-T and PolyHb-R demonstrated Hill coefficients of 1.0 ± 0.0 and 1.0 ± 0.1, respectively, while PDA-Poly-T and PDA-Poly-R demonstrated Hill coefficients of 0.9 ± 0.0 and 1.0 ± 0.1, respectively. The precursor hHb exhibited a Hill coefficient of

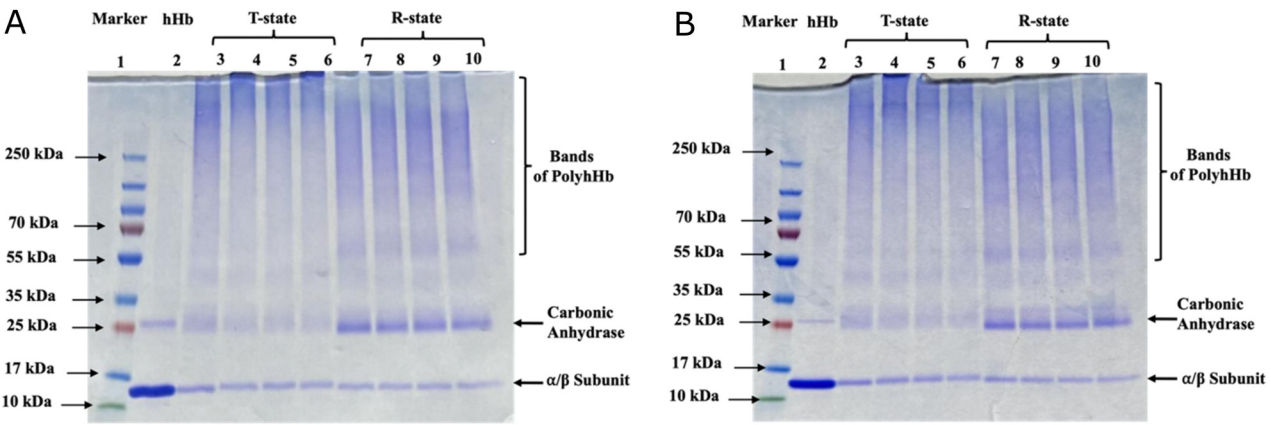

Fig. 3 SDS-PAGE analysis of the precursor hHb, T-state PolyHb, PDA-T-state PolyHb, R-state PolyHb, and PDA-R-state PolyHb under (A) non-denaturing conditions (without DTT) and (B) denaturing conditions (with DTT).

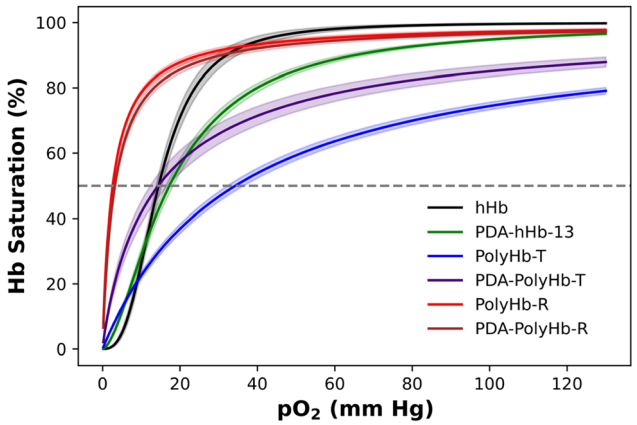

Fig. 4 Oxygen equilibrium curves for hHb, PDA–hHb-13, PolyHb-T, PDA–PolyHb-T, PolyHb-R, PDA–PolyHb-R at 37 °C and pH = 7.4.

2.8 ± 0.2, which decreased to 1.6 ± 0.0 upon PDA coating for PDA–hHb-13.[20]

3.7. Oxygen offloading kinetics

The kinetics of oxygen offloading were measured using UV-visible stopped-flow spectroscopy by monitoring the absorbance at 437.5 nm. PolyHb-T and PolyHb-R had oxygen offloading rate constants of 36.5 ± 0.2 s^{-1} and 14.1 ± 0.4 s^{-1} respectively, which are similar to those reported in the literature[12] (Fig. 5). Upon PDA coating, PolyHb-T exhibited a reduced oxygen offloading rate constant ($p < 0.001$), with PDA–PolyHb-T having a rate constant of 24.4 ± 1.6 s^{-1}. In comparison, there was no significant difference in the offloading rate constants of PDA–PolyHb-R and PolyHb-R ($p > 0.05$), with PDA–PolyHb-R exhibiting an offloading rate constant of 15.2 ± 0.7 s^{-1}. The precursor hHb had an oxygen offloading rate constant of 41.1 ± 0.8 s^{-1}, which remained unchanged upon PDA coating with PDA–hHb-13 exhibiting a rate constant of 41.3 ± 1.3 s^{-1} ($p > 0.05$).[20] Overall, the different groups followed similar trends for oxygen offloading rate constants and oxygen affinity, with the groups having higher P_{50} exhibiting higher oxygen offloading rate constants and *vice versa*.

3.8. Auto-oxidation kinetics

Auto-oxidation kinetics describe the rate of spontaneous oxidation of $HbFe^{2+}$ to $HbFe^{3+}$ and is measured by observing the absorption maximum at 630 nm corresponding to metHb. Both T- and R-state PolyHbs exhibited a significant increase in auto-oxidation rate constants upon PDA coating, with PDA–PolyHb-T and PDA–PolyHb-R exhibiting biphasic kinetics with a fast and a slow auto-oxidation rate constant (Fig. 6). PolyHb-T had a monophasic auto-oxidation rate constant of 0.0191 ± 0.0004 h^{-1}, while PDA–PolyHb-T had a fast auto-oxidation rate constant of 0.0848 ± 0.0095 h^{-1}, higher than that of PolyHb-T ($p < 0.01$), and slow auto-oxidation rate constant of 0.0164 ± 0.0019 h^{-1}, similar to that of PolyHb-T ($p > 0.05$). Similarly, PolyHb-R had a monophasic auto-oxidation rate constant of 0.0072 ± 0.0006 h^{-1}, whereas PDA–PolyHb-R had a fast auto-oxidation rate constant of 0.0201 ± 0.0003 h^{-1}, and slow auto-oxidation rate constant of 0.0094 ± 0.0002 h^{-1}. In comparison, the precursor hHb demonstrated a monophasic auto-oxidation rate constant of 0.008 ± 0.001 h^{-1}, which significantly increased upon PDA coating ($p < 0.001$). PDA–hHb-13 demonstrated a monophasic auto-oxidation rate constant of 0.078 ± 0.006 h^{-1}.[20]

3.9. Haptoglobin binding kinetics

The binding of haptoglobin (Hp) to the PolyHbs and the PDA-coated PolyHbs was assessed by measuring the fluorescence quenching of Hp due to the bound heme group (Fig. 7A and B). PolyHb-T and PolyHb-R had Hp binding rate constants (k_{Hp-Hb}) of 0.0058 ± 0.0007 μM^{-1} s^{-1} and 0.0040 ± 0.0001 μM^{-1} s^{-1}, which did not change significantly ($p > 0.05$) compared to the rate constants for PDA–PolyHb-T and PDA–PolyHb-R measured at 0.0048 ± 0.0004 μM^{-1} s^{-1} and 0.0036 ± 0.0002 μM^{-1} s^{-1} respectively. Similarly, k_{Hp-Hb} of hHb did not change significantly upon PDA coating ($p > 0.05$). hHb and PDA–hHb-13 had k_{Hp-Hb} of 0.15 ± 0.02 μM^{-1} s^{-1} and 0.16 ± 0.00 μM^{-1} s^{-1} respectively.[20]

3.10. Ferric reducing antioxidant power (FRAP) assay

The FRAP assay assesses the ability of a protein to reduce oxidizing agents and is a measure of a protein's antioxidant power. The assay analyzes the reduction of $HbFe^{3+}$ to $HbFe^{2+}$ by measuring the

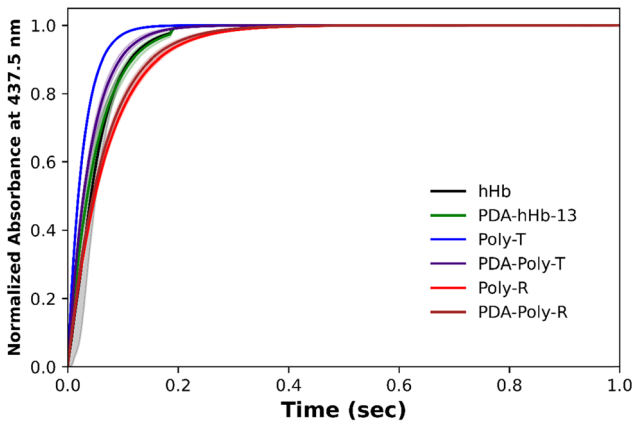

Fig. 5 Oxygen offloading kinetics of hHb, PDA–hHb-13, PolyHb-T, PDA–PolyHb-T, PolyHb-R, and PDA–PolyHb-R.

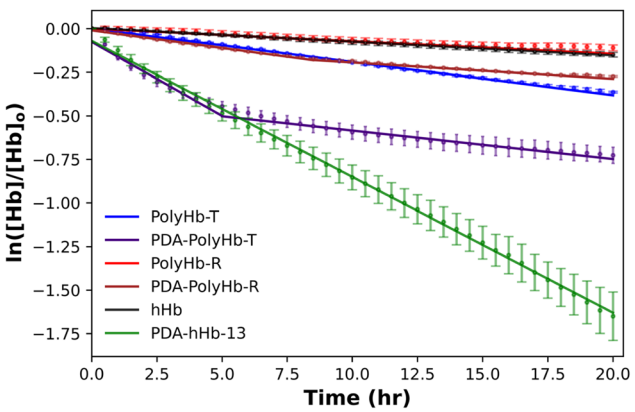

Fig. 6 Auto-oxidation kinetics of hHb, PDA–hHb-13, PolyHb-T, PDA–PolyHb-T, PolyHb-R, and PDA–PolyHb-R.

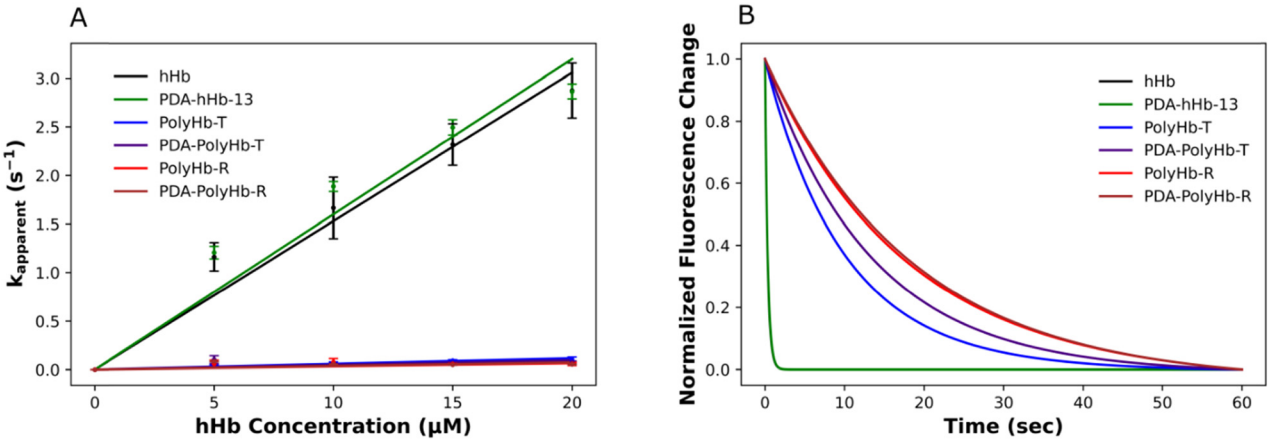

Fig. 7 (A) Representative average kinetic traces for hHb, PDA–hHb-13, PolyHb-T, PDA–PolyHb-T, PolyHb-R, and PDA–PolyHb-R binding to haptoglobin (Hp) at 0.25 μM. (B) Second order rate constant for Hp binding was obtained by plotting the pseudo-first order rate constants against protein concentration.

absorbance change at 593 nm. PolyHb-T and PolyHb-R had FRAP values of 10.4 ± 0.3 μM μg^{-1} and 9.3 ± 0.5 μM μg^{-1} of protein, respectively (Fig. 8). This means that PolyHb-T had the same FRAP activity as 10.4 ± 0.3 μM of ascorbic acid. Both PolyHbs showed a significant increase in FRAP activity upon PDA coating ($p < 0.001$) with PDA–PolyHb-T and PDA-Poly-R having FRAP values of 32.4 ± 1.3 μM μg^{-1} of protein and 21.3 ± 1.5 μM μg^{-1} of protein respectively. A similar trend of increased FRAP activity was observed for PDA coating of hHb ($p < 0.001$). The FRAP value for hHb was measured at 14.8 ± 0.5 μM μg^{-1}, while that for PDA–hHb-13 was measured at 31.5 ± 1.1 μM μg^{-1}.[20] These results confirm the successful incorporation of antioxidant properties upon PDA coating.

3.11. ABTS radical scavenging assay

The ABTS radical scavenging assay assesses the ability of a protein to scavenge reactive free radical species. The assay monitors the scavenging of $ABTS^{\bullet}$ by measuring the corresponding absorbance change at 734 nm, and the radical scavenging ability is reported as a % change in absorbance per μg of the protein added (Fig. 9). Both PolyHb-T and PolyHb-R demonstrated a significant increase in their radical scavenging activity upon PDA coating. The activity of PolyHb-T increased from 1.22 ± 0.07% μg^{-1} of protein to 3.05 ± 0.12% μg^{-1} of protein upon PDA coating ($p < 0.001$), while that for PolyHb-R increased from 1.06 ± 0.07% μg^{-1} of protein to 2.26 ± 0.12% μg^{-1} of protein ($p < 0.001$). A similar increase in radical scavenging was observed for hHb upon PDA coating. The radial scavenging activity of hHb was measured at 1.6 ± 0.1% μg^{-1}, which increased to 2.9 ± 0.1% μg^{-1} for PDA–hHb-13 ($p < 0.001$).[20] These results are consistent with previous studies related to PDA coating of proteins and are attributed to the quinone and catechol groups of the PDA coating that are implicated in electron transfer.[20,22,24]

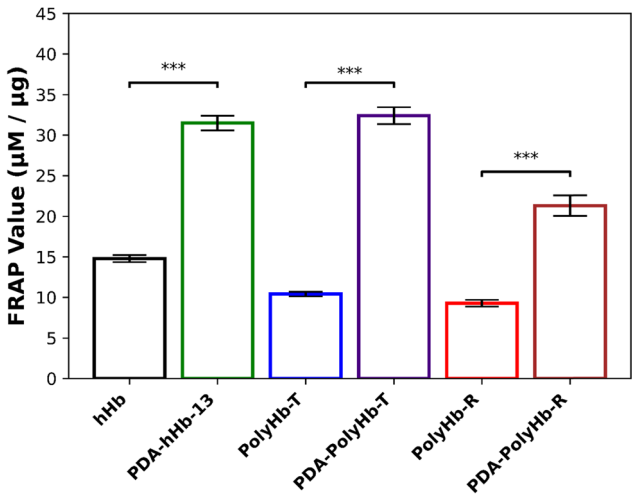

Fig. 8 Reducing power of proteins assessed by quantifying FRAP activity of hHb, PDA–hHb-13, PolyHb-T, PDA–PolyHb-T, PolyHb-R, and PDA–PolyHb-R.

3.12. Hydrogen peroxide mediated oxidation

Oxidation of ferrous (Fe^{2+}) and ferric (Fe^{3+}) Hb to ferryl Hb (Fe^{4+}) upon H_2O_2 addition was studied as a measure of antioxidant activity. $HbFe^{4+}$ is unstable and can further react with oxidizing agents to cause heme degradation.[16] Thus, the hydrogen peroxide mediated oxidation assay is a measure of antioxidant activity, and the low formation of sulfHb is desirable. We observed a significant decrease in sulfHb formation upon PDA coating for PolyHb-T ($p < 0.001$), with PolyHb-T generating a sulfHb of 13.0 ± 0.0 μM and PDA–PolyHb-T generating a sulfHb of 3.8 ± 0.4 μM due to oxidation by hydrogen peroxide (Fig. 10). PolyHb-R showed minimal sulfHb formation of 1.3 ± 0.1 μM, which was similar to the sulfHb generated by PDA-Poly-R, 1.3 ± 0.0 μM ($p > 0.05$). Interestingly, a different trend was observed for PDA coating of hHb, which showed higher sulfHb formation upon PDA coating ($p < 0.001$).[20] Sulfheme formation for hHb was measured at 0.3 ± 0.0 μM, whereas that for PDA–hHb-13 was measured at 6.6 ± 0.4 μM. This trend could be attributed to the higher catalase activity of hHb compared to

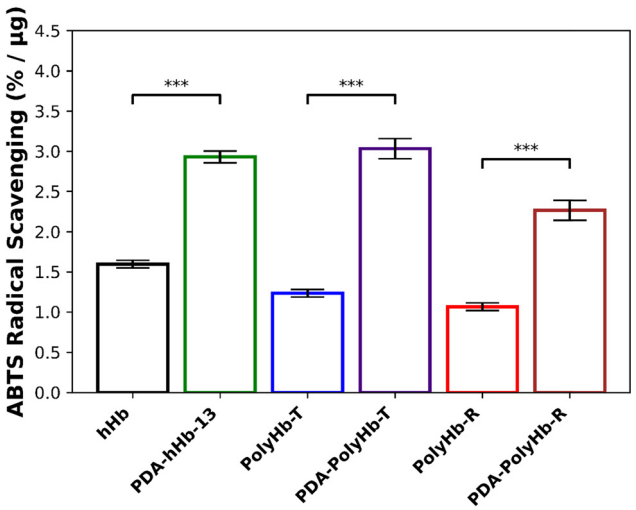

Fig. 9 Radical scavenging capacity of proteins assessed by quantifying ABTS radical scavenging activity of hHb, PDA–hHb-13, PolyHb-T, PDA–PolyHb-T, PolyHb-R, and PDA–PolyHb-R.

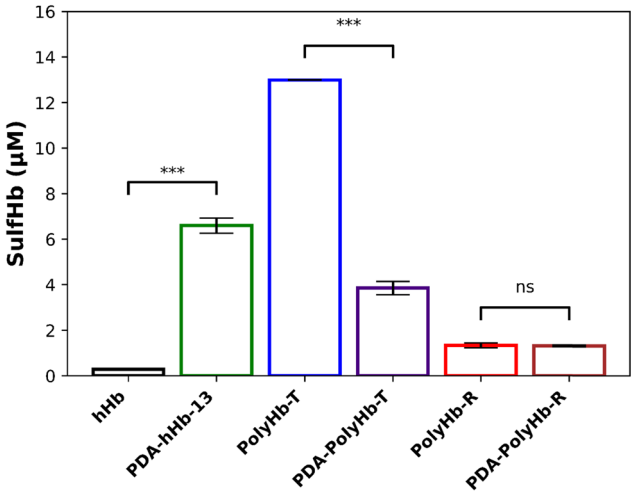

Fig. 10 Oxidation of hHb, PDA–hHb-13, PolyHb-T, PDA–PolyHb-T, PolyHb-R, and PDA–PolyHb-R to ferryl species, quantified by sulfHb formation.

PDA–hHb-13. The lower sulfHb formation for PolyHb-R is in agreement with our previous reports[12] and can be attributed to its high oxygen affinity.

3.13. Catalase activity assay

While the sulfHb assay measures the effect of H_2O_2 on the Fe atom in the heme group of Hb, the catalase activity assay measures the quenching of H_2O_2 in solution. The assay is performed by measuring the UV-visible absorbance of H_2O_2 at 240 nm and is reported as the activity of the enzyme catalase. We observed a significant increase in catalase activity for PolyHb-T upon PDA coating ($p < 0.05$), with PolyHb-T exhibiting an activity of 3.6 ± 0.5 units per mL and PDA–PolyHb-T exhibiting an activity of 5.2 ± 0.4 units per mL (Fig. 11). On the

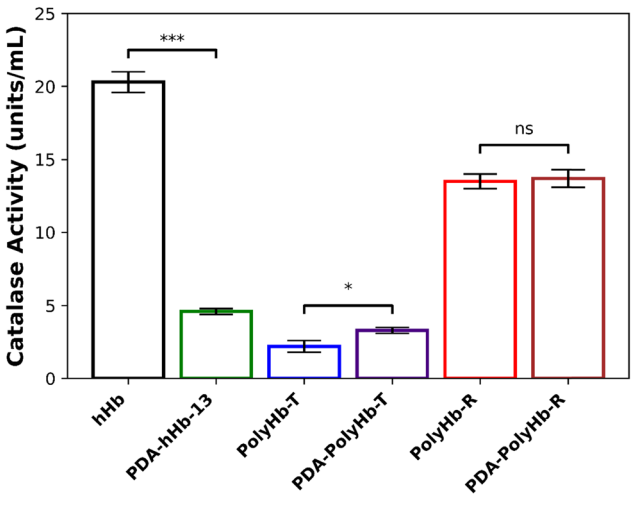

Fig. 11 Catalase activity quantification of hHb, PDA–hHb-13, PolyHb-T, PDA–PolyHb-T, PolyHb-R, and PDA–PolyHb-R.

other hand, PolyHb-R did not show an increased catalase activity upon PDA coating ($p > 0.05$). Catalase activity for PolyHb-R was measured at 21.4 ± 2.1 units per mL, and that for PDA-Poly-R was measured at 22.6 ± 0.8 units per mL. The precursor hHb exhibited a catalase activity of 20.3 ± 0.7 units per mL, which was higher than that for PDA–hHb-13 measured at 4.6 ± 0.2 units per mL ($p < 0.001$).[20] The catalase activity results correlate with the sulfHb assay results, where groups with higher catalase activity exhibit lower sulfHb formation due to H_2O_2-induced oxidation.

3.14. Circular dichroism spectroscopy

The impact of PDA coating on the secondary and tertiary structures of T- and R-state PolyHb was assessed using circular dichroism (CD) spectroscopy in the far-UV (190–260 nm) and near-UV (250–500 nm) regions, as shown in Fig. 12A and B. In the far-UV region, the CD spectra of the precursor hHb, PDA–hHb-13, T-state PolyHb, PDA-T-state PolyHb, R-state PolyHb, and PDA-R-state PolyHb exhibited characteristic α-helical protein features, displaying negative peaks at 208 and 222 nm. A significant difference in molar ellipticity at 222 nm ($p < 0.05$) was observed between T-state PolyHb and PDA-T-state PolyHb. In contrast, no significant difference in molar ellipticity at 222 nm ($p > 0.05$) was observed between R-state PolyHb and PDA-R-state PolyHb, as well as between hHb and PDA–hHb-13 ($p > 0.05$).[20]

In the near-UV region, all samples including, the precursor hHb, PDA–hHb-13, T-state PolyHb, PDA-T-state PolyHb, R-state PolyHb, and PDA-R-state PolyHb, displayed two characteristic positive peaks at approximately 260 and 420 nm. Monitoring the molar ellipticity at 420 nm, no statistically significant differences ($p > 0.05$) in spectral intensity were detected between uncoated and PDA-coated forms of either hHb, T- or R-state PolyHb. However, a slight reduction in molar ellipticity at 260 nm was observed for both PDA-T-state and PDA-R-state PolyHb compared to their respective uncoated counterparts

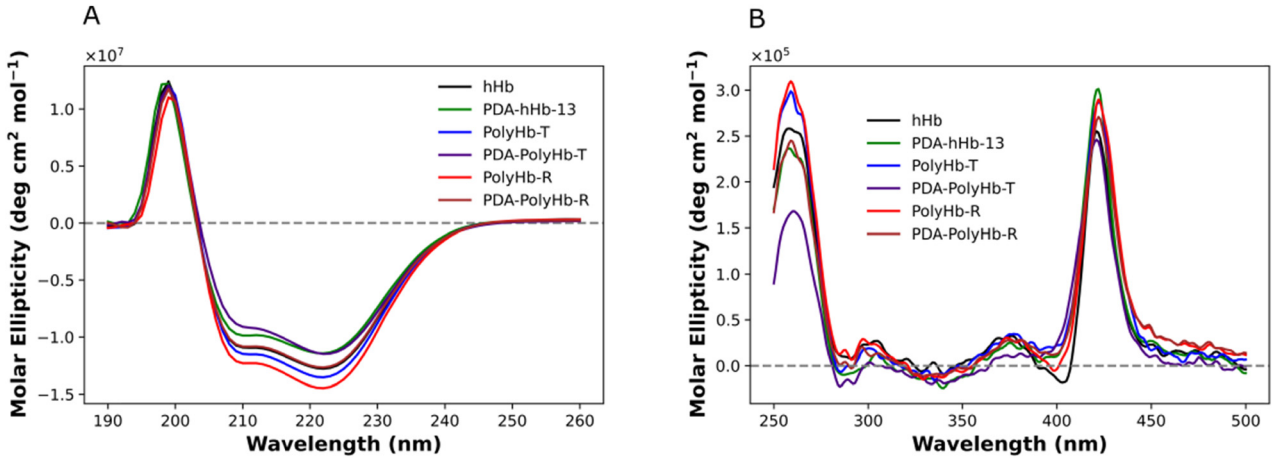

Fig. 12 (A) Far UV and (B) Near UV circular dichroism spectra of hHb, PDA–hHb-13, PolyHb-T, PDA–PolyHb-T, PolyHb-R, and PDA–PolyHb-R to assess changes in protein structure.

($p < 0.001$). Similarly, a significant difference was observed in the molar ellipticity of hHb and PDA–hHb-13 at 260 nm ($p < 0.01$).[20] Fig. 13 depicts the standard deviation in the molar ellipticity of the proteins at 222 nm, 260 nm and 420 nm.

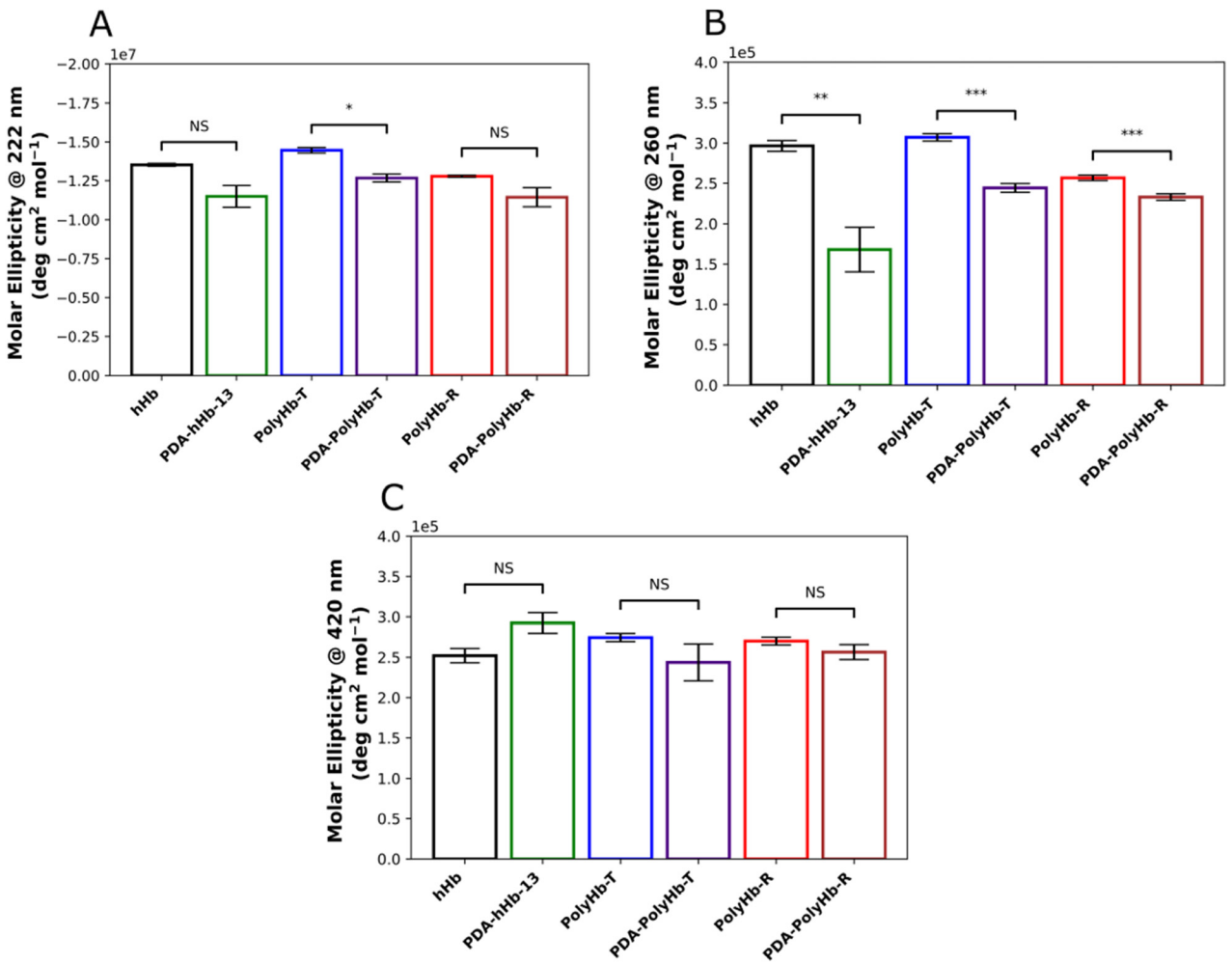

Fig. 13 Molar ellipticity of hHb, PDA–hHb-13, PolyHb-T, PDA–PolyHb-T, PolyHb-R, and PDA–PolyHb-R at (A) 222 nm, (B) 260 nm, and (C) 420 nm.

3.15. Thermal stability

The thermal stability of the precursor hHb, T- and R-state PolyHb, and PDA-coated T- and R-state PolyHb samples was evaluated using circular dichroism (CD) spectroscopy over a range of temperatures (20 °C to 90 °C) (Fig. 14). Protein unfolding curves were obtained by plotting the normalized ellipticity at 222 nm as a function of temperature, allowing determination of the midpoint transition temperature (T_m). The calculated T_m values, representing the thermal stability of each hHb variant, are presented in Table 1. The precursor hHb displayed a T_m of 65.9 ± 0.2 °C, while[12] T- and R-state PolyHb exhibited T_m values of 73.9 ± 0.7 °C and 78.1 ± 1.3 °C, respectively, corresponding to increases of 8.0 °C and 12.2 °C on average relative to unmodified hHb, consistent with previously published data.[12] PDA coating of hHb resulted in a slight decrease in thermal stability, with PDA–hHb-13 exhibiting a T_m of 59.3 ± 0.2 °C ($p < 0.001$).[20] Similarly, PDA coating of the T-state PolyHb led to a modest yet statistically significant reduction in thermal stability, yielding a T_m of 71.3 ± 0.8 °C compared to uncoated T-state PolyHb ($p < 0.05$). For R-state PolyHb, PDA modification produced a T_m of 76.0 ± 1.4 °C, showing no statistically significant difference from uncoated R-state PolyHb ($p > 0.05$). The decrease in T_m upon PDA coating is consistent with our study on PDA–hHb, where PDA coating resulted in a modest decrease in the T_m of hHb.

4. Discussion

In our previous work, we developed PDA-coated hHb and found that CO-binding the hHb before application of the PDA coating significantly reduced metHb formation.[20] At the same time, although PDA-coating using pre-formed PDA NPs led to significantly lower auto-oxidation rates, the resultant particle size was too large. Because the PDA coating is biodegradable, the use of PDA–hHb in transfusion medicine could lead to potential exposure to hHb, which has been proven to be toxic.[26,27] Therefore, in this work, we explore PDA coating of T- and R-state PolyHbs that have shown safety in animal models.[31,39,40] We did not implement the method of using pre-formed PDA NPs in order to obtain a particle size less than 0.2 μm for PDA–PolyHb. However, CO-locking was found to significantly reduce metHb formation in both PDA-coated T- and R-state PolyHb.

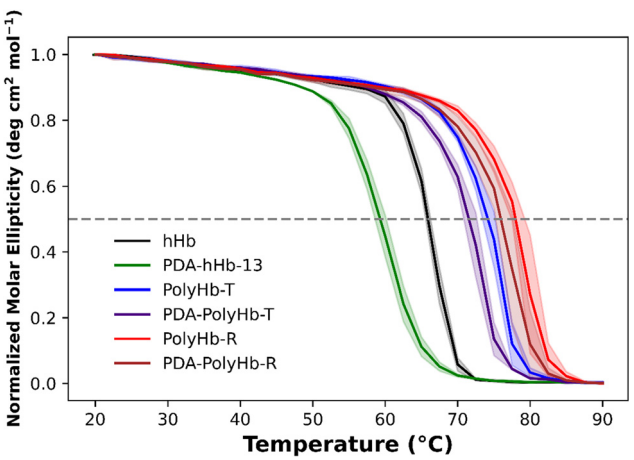

Fig. 14 Thermal stability quantification of hHb, PDA–hHb-13, PolyHb-T, PDA–PolyHb-T, PolyHb-R, and PDA–PolyHb-R.

An increase in the hydrodynamic diameter of both the PolyHbs was observed upon PDA coating and can be attributed to the contribution of the thickness of the PDA coating to the particle diameter. This observation is consistent with other studies reported in the literature, as well as our study on PDA–hHb, where an increase in particle diameter upon PDA coating was observed for PDA–hHb-13.[20,24] PolyHb consists of multiple polymeric species, with sizes ranging from 500 kDa to 0.2 μm,[35] contributing to a high PDI as reported in this study. PDA coating of PolyHb in this study involved the simultaneous addition of CO-bound PolyHb with dopamine at a basic pH, and no significant difference in the PDI of PolyHbs and their corresponding PDA–PolyHbs was observed. These results are consistent with our previous study on PDA coating of hHb, where PDA coating involving simultaneous addition of hHb and dopamine did not result in a significantly different PDI for PDA–hHb-13.[20]

To study whether PDA coating affected the oxygen transport properties of PolyHbs, we studied the oxygen affinity and oxygen offloading kinetics. Interestingly, there was an increase in the oxygen affinity of PolyHb-T upon PDA coating, whereas PolyHb-R exhibited a slight decrease in its oxygen affinity upon PDA coating. In our previous study on the PDA coating of Hb, PDA–hHb-13 demonstrated a slight decrease in its oxygen affinity, likely due to the interaction of dopamine with the central water cavity.[20] In a study involving molecular docking simulations performed by Nadimifar *et al.*, it was found that dopamine can interact with the heme pocket and the central water cavity due to the PDA coating, which could alter the oxygen affinity of PolyHbs.[20,41] In addition, PDA contains catechol, quinone, and amine groups that can form hydrogen bonds, electrostatic interactions, or weak covalent linkages with Hb surface residues such as lysines, cysteines, and tyrosines exposed in PolyHb-T. These interactions could possibly lock structural elements that favor the O_2-bound geometry or restrict conformational fluctuations that facilitate O_2 release. Both PolyHbs had a Hill coefficient (n) of about 1, indicating the absence of cooperative oxygen binding among the heme subunits. This is a characteristic of polymerized Hbs and arises from conformational restrictions due to crosslinking. We expect a reduction in cooperativity upon PDA coating based on previous studies, with PDA–hHb-13 demonstrating a reduced cooperativity compared to hHb.[20,24] However, because the PolyHbs already had an absence of cooperativity, further changes were not observed after PDA coating. The rate of oxygen offloading correlated with the oxygen affinity for all materials, as expected from previous studies.[42] Materials with higher P_{50} (lower oxygen affinity) corresponded to higher oxygen offloading rate constants.

The objective of this work was to impart antioxidant properties to PolyHbs *via* the PDA coating. Thus, to investigate whether there was an increase in antioxidant activity, we employed the FRAP,

ABTS, catalase activity, and sulfHb formation assays. The FRAP and ABTS assays describe the reducing power and the radical scavenging capacity of the different materials. We observed a significant increase in both properties for PDA–PolyHb-T and PDA–PolyHb-R, compared to PolyHb-T and PolyHb-R respectively, and this increase is attributed to the redox active quinone and catechol groups of PDA.[43] This increase is in alignment with our previous study, where PDA–hHb-13 showed increased reducing power and radical scavenging activity compared to hHb.[20] Similar observations have been reported by several other studies involving PDA coating of proteins.[20,22,24]

H_2O_2 is a common ROS and therefore, resistance to H_2O_2 oxidation was studied using the catalase activity and sulfHb formation assays. The catalase activity assay quantifies the quenching of H_2O_2, while the sulfHb formation assay quantifies the oxidative damage to Hb due to H_2O_2. There was a significant increase in catalase activity, as well as a significant decrease in sulfHb formation for PDA-Poly-T compared to Poly-T, highlighting antioxidant protection due to the PDA coating. Interestingly, PolyHb-R had high antioxidant protection against H_2O_2, which was not significantly changed upon PDA coating. The low sulfHb formation for PolyHb-R and PDA–PolyHb-R could be explained by their high oxygen affinity. Oxidation of $HbFe^{2+}$ involves the release of O_2, which could cause groups with a high oxygen affinity to have lower sulfHb formation.[16] The precursor hHb contains the enzyme catalase from the RBC lysate, contributing to its high catalase activity. This co-purified catalase likely loses its enzymatic activity during the process of PDA coating, leading to PDA–hHb-13 having lower catalase activity. Overall, the catalase activity and sulfHb formation results support each other, with materials having higher catalase activity exhibiting lower sulfHb formation.

Physiologically, cell-free Hb is eliminated from the circulation *via* the reticuloendothelial system (mainly the liver and spleen), *via* Hp-mediated macrophage uptake, and Hb dimers are eliminated through renal filtration.[27,44,45] Thus, the Hp-binding kinetics study provides insight into the potential rate of elimination of HBOCs *via* the Hp-mediated pathway. Hp binds to Hb dimers significantly faster than Hb tetramers and polymers, due to steric hindrance.[46] Therefore, we have previously observed significantly lower rates of Hp-binding for T- and R-state PolyHbs compared to the precursor hHb.[12] The T- and R-state PolyHbs evaluated in this study also exhibited extremely low Hp-binding rate constants, which remained unchanged after PDA coating.

SDS-PAGE analysis of both T- and R-state PolyHb and their PDA-coated counterparts revealed faint bands near ~16 kDa, corresponding to uncross-linked α and β subunits. The presence of these minor bands may result from partial dissociation of PolyHb species under the harsh denaturing conditions employed during electrophoresis, both with and without DTT. Bands appearing around ~30–32 kDa are likely attributed to carbonic anhydrase (~30 kDa), which is known to be present as a residual impurity since the hHb precursor exhibits approximately 98% purity.[12] Despite these minor bands, all samples displayed similar high MW bands, and no distinct differences were observed between uncoated and PDA-coated forms. This finding indicates that PDA modification does not promote further polymer dissociation, confirming that the polymerized structure remains stable and intact following coating.

The structural effects of PDA coating on T- and R-state PolyHb were further examined using CD spectroscopy. Far-UV spectra confirmed that all variants retained predominantly α-helical secondary structures. A slight decrease in molar ellipticity was observed for PDA-coated T-state PolyHb compared to the uncoated T-state PolyHb, suggesting minor perturbations to the protein backbone and a modest loss of α-helical content due to PDA coating. In contrast, hHb and R-state PolyHb exhibited minimal structural changes after PDA modification, indicating preservation of their secondary structure. In the near-UV region, molar ellipticity measurements at 420 nm showed no significant differences between uncoated and PDA-coated samples for hHb, T- and R-state PolyHb. This consistency suggests that the heme prosthetic group remained securely integrated within the globin chains and that the local heme pocket environment was largely unaffected by PDA coating. However, a slight reduction in molar ellipticity at 260 nm was detected in both PDA-coated T- and R-state PolyHb compared to their uncoated counterparts, indicating minor alterations in tertiary structure. These lower ellipticity values imply a slightly less rigid or more loosely packed aromatic environment, likely reflecting subtle conformational rearrangements induced by the PDA coating process. In comparison, there was no change in the molar ellipticity at 260 nm for hHb and PDA–hHb-13, indicating preservation of their tertiary structure. PDA-coated hHb and T-state PolyHb exhibited a moderate yet statistically significant decrease in T_m, compared to their uncoated precursors. This reduction may result from mild disruption of protein conformation, consistent with the small loss in α-helical content observed in the far-UV spectra. Conversely, R-state PolyHb displayed no significant difference in T_m from the uncoated R-state PolyHb. This aligns with the far-UV CD spectra results, confirming that the R-state PolyHb conformation remains structurally stable following PDA modification.

Interestingly, we observe different trends in changes in the oxygen transport properties of T-state PolyHb compared to that of R-state PolyHb upon PDA coating. R-state PolyHb experiences minor changes in its oxygen affinity and oxygen offloading rate constant, whereas T-state PolyHb experiences significant changes in both of these properties. T- and R-state PolyHb have different conformations, which could impact how polydopamine interacts with the heme pocket. It would be interesting to study these interactions with the help of a molecular docking approach, similar to the one employed by Nadimifar *et al.* to study the interactions of dopamine and polydopamine with Hb.[41]

T- and R-state PolyHb each have different intended applications based on owing to their oxygen binding properties. T-state PolyHb has a low oxygen affinity and is desirable for hemorrhagic shock resuscitation.[40] Comparatively, R-state PolyHb has a high oxygen affinity and has applications in oxygenating the tumor micro-environment which is severely hypoxic.[15] We ideally prefer to develop a PDA-coating method that would

impart antioxidant properties to HBOCs without significantly altering their oxygen transport properties. This is desirable so that HBOCs can be developed independently and a PDA-coating can be imparted to them as a secondary functionality. In this regard, further investigation is needed to modify the PDA-coating method such that the oxygen transport properties of T-state PolyHb are not significantly altered due to the PDA coating.

5. Conclusion

This study successfully introduced antioxidant properties to T- and R-state PolyHb *via* PDA coating, thus enabling O_2 transport and protection against oxidative stress. FRAP activity and radical scavenging activity were increased upon PDA coating for both T- and R-state PolyHb, while notable improvements in catalase activity and sulfHb formation were only observed for T-state PolyHb. R-state PolyHb retained its oxygen transport characteristics, whereas there was a significant increase in the oxygen affinity of T-state PolyHb upon PDA coating, and a corresponding decrease in its oxygen offloading rate constant. Auto-oxidation rate constants significantly increased for both PolyHbs upon PDA coating. However, the magnitude of the increase was lower compared to that of hHb upon PDA coating *via* the same method. These changes are likely due to alterations in the heme pocket environment due to the binding of dopamine in the heme pocket. An increase in hydrodynamic diameter was observed for both PolyHbs upon PDA coating without affecting polydispersity indices. SDS-PAGE analysis confirmed that the PDA coating did not induce PolyHb dissociation and preserved the structural integrity of all PolyHb variants. PDA coating maintained the α-helical and tertiary structures of both T- and R-state PolyhHb, with slight changes for PDA–PolyHb-T. Polymerization improved thermal stability compared to native hHb, whereas PDA modification caused a slight reduction in the stability of T-state PolyHb without affecting R-state PolyHb. Overall, these results demonstrate that PDA-coated T- and R-state PolyhHb possess enhanced antioxidant capacity, structural stability, and oxygen-carrying functionality, indicating strong potential as next-generation hemoglobin-based oxygen carriers (HBOCs) for potential therapeutic use in hypoxic conditions and hemorrhagic shock treatment.

Author contributions

Tanmay Salvi: writing – original draft, conceptualization, methodology, investigation. Mohd Asim Khan: writing – original draft, conceptualization, methodology, investigation. Peyton Dickerson: investigation. Griffin J. Beyer: investigation. Andre F. Palmer: writing – review & editing, resources, funding acquisition.

Conflicts of interest

A. F. P. is an inventor on US patent application # PCT/US2023/079410 that describes the synthesis of PDA encapsulated Hb.

Data availability

Data will be made available upon request.

Acknowledgements

This work was supported by National Institutes of Health grant R01HL156526. We acknowledge the Biophysical Interaction and Characterization Facility (BICF) in the Chemical and Biomolecular Engineering Department at The Ohio State University for using their CD spectrometer.

References

1 S. A. Glynn, M. P. Busch, G. B. Schreiber, E. L. Murphy, D. J. Wright, Y. Tu, S. H. Kleinman and N. R. S. Group, Effect of a national disaster on blood supply and safety: the September 11 experience, *JAMA*, 2003, **289**(17), 2246–2253, DOI: 10.1001/jama.289.17.2246.

2 M. T. Ayyoubi, T. Konstenius, J. C. McCullough, T. Eastlund, M. Clay, R. Bowman, A. M. Rahmani, W. Riley and J. McCullough, Status of blood banking and the blood supply in Afghanistan, *Transfusion*, 2010, **50**(3), 566–574, DOI: 10.1111/j.1537-2995.2009.02485.x.

3 O. Baidukova, Q. Wang, S. Chaiwaree, D. Freyer, A. Prapan, R. Georgieva, L. Zhao and H. Bäumler, Antioxidative protection of haemoglobin microparticles (HbMPs) by PolyDopamine, *Artif. Cells, Nanomed., Biotechnol.*, 2018, **46**(sup3), S693–S701, DOI: 10.1080/21691401.2018.1505748.

4 R. Hickey and A. F. Palmer, Synthesis of Hemoglobin-Based Oxygen Carrier Nanoparticles by Desolvation Precipitation, *Langmuir*, 2020, **36**(47), 14166–14172, DOI: 10.1021/acs.langmuir.0c01698.

5 X. Gu, C. Savla and A. F. Palmer, Tangential flow filtration facilitated fractionation and PEGylation of low and high-molecular weight polymerized hemoglobins and their biophysical properties, *Biotechnol. Bioeng.*, 2022, **119**(1), 176–186, DOI: 10.1002/bit.27962.

6 X. Gu and A. F. Palmer, ZIF-8 Metal–Organic Framework Nanoparticles Loaded with Hemoglobin as a Potential Red Blood Cell Substitute, *ACS Appl. Nano Mater.*, 2022, **5**(4), 5670–5679, DOI: 10.1021/acsanm.2c00608.

7 H. Sakai, Translational Research of Hemoglobin-vesicles as a Transfusion Alternative, in *Advanced Materials - TechConnect Briefs*, TechConnect, 2016, Vol. 3, pp. 69–70, DOI: 10.2174/092986732866210412130035.

8 Y. Iwashita, Relationship between chemical properties and biological properties of pyridoxalated hemoglobin-polyoxyethylene, *Biomater., Artif. Cells, Immobilization Biotechnol.*, 1992, **20**(2–4), 299–307, DOI: 10.3109/10731199209119647.

9 J. S. Jahr, N. R. Guinn, D. R. Lowery, L. Shore-Lesserson and A. Shander, Blood Substitutes and Oxygen Therapeutics: A Review, *Anesth. Analg.*, 2021, **132**(1), 119–129, DOI: 10.1213/ANE.0000000000003957.

10 P. Cabrales, G. Sun, Y. Zhou, D. R. Harris, A. G. Tsai, M. Intaglietta and A. F. Palmer, Effects of the molecular mass of tense-state polymerized bovine hemoglobin on blood pressure and vasoconstriction, *J. Appl. Physiol.*, 2009, **107**(5), 1548–1558, DOI: 10.1152/japplphysiol.00622.2009.

11 C. T. Cuddington, S. R. Wolfe and A. F. Palmer, Biophysical properties of tense quaternary state polymerized human hemoglobins bracketed between 500 kDa and 0.2 μm in size, *Biotechnol. Prog.*, 2022, **38**(1), 1–8, DOI: 10.1002/btpr.3219.

12 M. A. Khan, T. Salvi, G. J. Beyer, A. Abdalbaqi, M. Allyn, A. Bresolin, A. F. Palmer and on behalf of the CONCERT research program, Scalable Production and Biophysical Characterization of High-Molecular-Weight Relaxed and Tense Quaternary State Polymerized Human Hemoglobin as Potential Red Blood Cell Substitutes, *Biomacromolecules*, 2024, **25**(11), 7334–7348, DOI: 10.1021/acs.biomac.4c01024.

13 M. A. Khan, G. J. Beyer, T. Salvi and A. F. Palmer, Biophysical and Biochemical Characterization of PEGylated High-Molecular-Weight Relaxed and Tense Quaternary State Polymerized Human Hemoglobin, *Bioconjugate Chem.*, 2025, **36**(9), 2020–2036, DOI: 10.1021/acs.bioconjchem.5c00311.

14 C. R. Muller, V. Courelli, C. Walser, C. T. Cuddington, S. R. Wolfe, A. F. Palmer and P. Cabrales, Polymerized human hemoglobin with low and high oxygen affinity in trauma models, *Transl. Res.*, 2023, **260**, 83–92, DOI: 10.1016/j.trsl.2023.05.006.

15 D. A. Belcher, A. Lucas, P. Cabrales and A. F. Palmer, Polymerized human hemoglobin facilitated modulation of tumor oxygenation is dependent on tumor oxygenation status and oxygen affinity of the hemoglobin-based oxygen carrier, *Sci. Rep.*, 2020, **10**(1), 11372, DOI: 10.1038/s41598-020-68190-0.

16 E. Nagababu, S. Ramasamy, J. M. Rifkind, Y. Jia and A. I. Alayash, Site-Specific Cross-Linking of Human and Bovine Hemoglobins Differentially Alters Oxygen Binding and Redox Side Reactions Producing Rhombic Heme and Heme Degradation, *Biochemistry*, 2002, **41**(23), 7407–7415, DOI: 10.1021/bi0121048.

17 C. Fleury, B. Mignotte and J. L. Vayssiere, Mitochondrial reactive oxygen species in cell death signaling, *Biochimie*, 2002, **84**(2–3), 131–141, DOI: 10.1016/s0300-9084(02)01369-x.

18 F. D'Agnillo and T. M. Chang, Polyhemoglobin-superoxide dismutase-catalase as a blood substitute with antioxidant properties, *Nat. Biotechnol.*, 1998, **16**(7), 667–671, DOI: 10.1038/nbt0798-667.

19 J. Chen, X. Liu, M. M. T. Jansman, P. W. Thulstrup and L. Hosta-Rigau, Metal-Phenolic Networks as Broad-Spectrum Antioxidant Coatings for Hemoglobin Nanoparticles Working as Oxygen Carriers, *Chem. Mater.*, 2022, **34**(20), 9200–9211, DOI: 10.1021/acs.chemmater.2c02190.

20 T. Salvi, M. A. Khan, G. J. Beyer and A. F. Palmer, Comprehensive biophysical and biochemical characterization of polymerized dopamine coated hemoglobin based oxygen carrier, *Int. J. Biol. Macromol.*, 2025, **322**(Pt 1), 146658, DOI: 10.1016/j.ijbiomac.2025.146658.

21 J. Hu, Q. Wang, Y. Wang, G. You, P. Li, L. Zhao and H. Zhou, Polydopamine-based surface modification of hemoglobin particles for stability enhancement of oxygen carriers, *J. Colloid Interface Sci.*, 2020, **571**, 326–336, DOI: 10.1016/j.jcis.2020.03.046.

22 Q. Wang, R. Zhang, M. Lu, G. You, Y. Wang, G. Chen, C. Zhao, Z. Wang, X. Song and Y. Wu, *et al.*, Bioinspired Polydopamine-Coated Hemoglobin as Potential Oxygen Carrier with Antioxidant Properties, *Biomacromolecules*, 2017, **18**(4), 1333–1341, DOI: 10.1021/acs.biomac.7b00077.

23 Q. Wang, R. Zhang, G. You, J. Hu, P. Li, Y. Wang, J. Zhang, Y. Wu, L. Zhao and H. Zhou, Influence of polydopamine-mediated surface modification on oxygen-release capacity of haemoglobin-based oxygen carriers, *Artif. Cells, Nanomed., Biotechnol*, 2018, **46**(sup2), 484–492, DOI: 10.1080/21691401.2018.1459636.

24 E. Pozy, C. Savla and A. F. Palmer, Photocatalytic Synthesis of a Polydopamine-Coated Acellular Mega-Hemoglobin as a Potential Oxygen Therapeutic with Antioxidant Properties, *Biomacromolecules*, 2023, **24**(5), 2022–2029, DOI: 10.1021/acs.biomac.2c01420.

25 J. Chen, M. M. T. Jansman, X. Liu and L. Hosta-Rigau, Synthesis of Nanoparticles Fully Made of Hemoglobin with Antioxidant Properties: A Step toward the Creation of Successful Oxygen Carriers, *Langmuir*, 2021, **37**(39), 11561–11572, DOI: 10.1021/acs.langmuir.1c01855.

26 P. Jiang, A. Choi and K. E. Swindle-Reilly, Controlled release of anti-VEGF by redox-responsive polydopamine nanoparticles, *Nanoscale*, 2020, **12**(33), 17298–17311, DOI: 10.1039/d0nr03710a.

27 J. P. Savitsky, J. Doczi, J. Black and J. D. Arnold, A clinical safety trial of stroma-free hemoglobin, *Clin. Pharmacol. Ther.*, 1978, **23**(1), 73–80, DOI: 10.1002/cpt197823173.

28 H. W. Kim and A. G. Greenburg, Ferrrous hemoglobin scavenging of endothelium derived nitric oxide is a principal mechanism for hemoglobin mediated vasoactivities in isolated rat thoracic aorta, *Artif. Cells, Blood Substitutes, Biotechnol.*, 1997, **25**(1–2), 121–133, DOI: 10.3109/10731199709118904.

29 C. R. Muller, V. Courelli, A. Lucas, A. T. Williams, J. B. Li, F. Dos Santos, C. T. Cuddington, S. R. Moses, A. F. Palmer and E. B. Kistler, *et al.*, Resuscitation from hemorrhagic shock after traumatic brain injury with polymerized hemoglobin, *Sci. Rep.*, 2021, **11**(1), 2509, DOI: 10.1038/s41598-021-81717-3.

30 C. R. Muller, A. T. Williams, C. J. Munoz, A. M. Eaker, A. N. Breton, A. F. Palmer and P. Cabrales, Safety profile of high molecular weight polymerized hemoglobins, *Transfusion*, 2021, **61**(1), 212–224, DOI: 10.1111/trf.16157.

31 C. R. Muller, A. T. Williams, C. Walser, A. M. Eaker, J. L. Sandoval, C. T. Cuddington, S. R. Wolfe, A. F. Palmer and P. Cabrales, Safety and efficacy of human polymerized hemoglobin on guinea pig resuscitation from hemorrhagic shock, *Sci. Rep.*, 2022, **12**(1), 1–12, DOI: 10.1038/s41598-022-23926-y.

32 D. Liu, A. Mori and L. Huang, Role of liposome size and RES blockade in controlling biodistribution and tumor uptake

of GM1-containing liposomes, *Biochim. Biophys. Acta*, 1992, **1104**(1), 95–101, DOI: 10.1016/0005-2736(92)90136-a.

33 A. F. Palmer, G. Sun and D. R. Harris, Tangential flow filtration of hemoglobin, *Biotechnol. Prog.*, 2009, **25**(1), 189–199, DOI: 10.1002/btpr.119.

34 D. R. Arifin and A. F. Palmer, Determination of size distribution and encapsulation efficiency of liposome-encapsulated hemoglobin blood substitutes using asymmetric flow field-flow fractionation coupled with multi-angle static light scattering, *Biotechnol. Prog.*, 2003, **19**(6), 1798–1811, DOI: 10.1021/bp034120x.

35 C. T. Cuddington, S. R. Wolfe, D. A. Belcher, M. Allyn, A. Greenfield, X. Gu, R. Hickey, S. Lu, T. Salvi and A. F. Palmer, Pilot scale production and characterization of next generation high molecular weight and tense quaternary state polymerized human hemoglobin, *Biotechnol. Bioeng.*, 2022, **119**(12), 3447–3461, DOI: 10.1002/bit.28233.

36 I. F. F. Benzie and M. Devaki, The ferric reducing/antioxidant power (FRAP) assay for non-enzymatic antioxidant capacity: Concepts, procedures, limitations and applications, *Measurement of Antioxidant Activity and Capacity: Recent Trends and Applications*, 2017, pp. 77–106, DOI: 10.1002/9781119135388.ch5.

37 R. Re, N. Pellegrini, A. Proteggente, A. Pannala, M. Yang and C. Rice-Evans, Antioxidant activity applying an improved ABTS radical cation decolorization assay, *Free Radicals Biol. Med.*, 1999, **26**(9–10), 1231–1237, DOI: 10.1016/S0891-5849(98)00315-3.

38 F. Meng, T. Kassa, S. Jana, F. Wood, X. Zhang, Y. Jia, F. D'Agnillo and A. I. Alayash, Comprehensive Biochemical and Biophysical Characterization of Hemoglobin-Based Oxygen Carrier Therapeutics: All HBOCs Are Not Created Equally, *Bioconjugate Chem.*, 2018, **29**(5), 1560–1575, DOI: 10.1021/acs.bioconjchem.8b00093.

39 C. R. Muller, V. Courelli, A. Lucas, A. T. Williams, J. B. Li, F. Dos Santos, C. T. Cuddington, S. R. Moses, A. F. Palmer and E. B. Kistler, *et al.*, Resuscitation from hemorrhagic shock after traumatic brain injury with polymerized hemoglobin, *Sci. Rep.*, 2021, **11**(1), 1–11, DOI: 10.1038/s41598-021-81717-3.

40 C. R. Muller, V. Courelli, C. Walser, C. T. Cuddington, S. R. Wolfe, A. F. Palmer and P. Cabrales, Polymerized human hemoglobin with low and high oxygen affinity in trauma models, *Transl. Res.*, 2023, **260**(2022), 83–92, DOI: 10.1016/j.trsl.2023.05.006.

41 M. Nadimifar, H. Ghourchian, L. Hosta-Rigau and A. A. Moosavi-Movahedi, Structural and functional alterations of polydopamine-coated hemoglobin: New insights for the development of successful oxygen carriers, *Int. J. Biol. Macromol.*, 2023, 253, DOI: 10.1016/j.ijbiomac.2023.127275.

42 X. Gu, C. Savla and A. F. Palmer, Tangential flow filtration facilitated fractionation and PEGylation of low and high-molecular weight polymerized hemoglobins and their biophysical properties, *Biotechnol. Bioeng.*, 2022, **119**(1), 176–186, DOI: 10.1002/BIT.27962.

43 E. Kim, M. Kang, T. Tschirhart, M. Malo, E. Dadachova, G. Cao, J. J. Yin, W. E. Bentley, Z. Wang and G. F. Payne, Spectroelectrochemical Reverse Engineering DemonstratesThat Melanin's Redox and Radical Scavenging Activities Are Linked, *Biomacromolecules*, 2017, **18**(12), 4084–4098, DOI: 10.1021/acs.biomac.7b01166.

44 H. F. Bunn, W. T. Esham and R. W. Bull, The renal handling of hemoglobin: I. Glomerular filtration, *J. Exp. Med.*, 1969, **129**(5), 909–924.

45 T. N. Estep, Pharmacokinetics and mechanisms of plasma removal of hemoglobin-based oxygen carriers, *Artif. Cells, Nanomed., Biotechnol.*, 2015, **43**(3), 203–215, DOI: 10.3109/21691401.2015.1047501.

46 D. A. Belcher, C. T. Cuddington, E. L. Martindale, I. S. Pires and A. F. Palmer, Controlled Polymerization and Ultrafiltration Increase the Consistency of Polymerized Hemoglobin for Use as an Oxygen Carrier, *Bioconjugate Chem.*, 2020, **31**(3), 605–621, DOI: 10.1021/acs.bioconjchem.9b00766.